Design and calculation method for Dynamic Increasing Transmission Line Capacity

LIJIA REN, XIUCHEN JIANG, GEHAO SHENG, WU BO
Department of Electric Engineering
Shanghai Jiaotong University
Shanghai 200240
CHINA
ljren@sjtu.edu.cn http://www.sjtu.edu.cn

Abstract: - The Dynamic Line Rating (DLR) system is designed to improve the transmission capacity of overhead lines, which decreases or delays to re-build transmission lines. The system is composed of sampling terminals installed on dead-end configuration of a line and one control instrument equipped in dispatch center. The data between the sampling terminals and the control instrument is transmitted through GPRS/GSM. Through Ethernet, the control instrument exchanges data with SCADA interface in order to integrate DLR and SCADA system. A solar Photovoltaic (PV) power supply system based on Perturb & Observe MPPT techniques was designed and successfully applied to outdoor on-line monitoring DLR system. The paper analyzed mechanical actions for overhead line concerned wind speeds and wind direction in a deflection plane. The force balance for overhead line in wind was analyzed in detail, which deduces the mechanical model to calculate sags from the measured tension. Overhead line's state equation was corrected used the relation of temperature and sags, and deduced the ultimately line's temperature. Analyzed the advantages and drawbacks of some mathematical model used to calculate transmission capacity. In order that the DLR system received the optimum dynamic capacity curve, combined the WM and TS model. The result shows that the DLR system is effective in increasing line capacity without violating the legal ground clearance, monitoring the on-line parameters of transmission lines, and insuring the safe ground clearances of transmission line at all times.

Key-Words: - Dynamic Line Rating (DLR); Transmission line; Transmission capacity; Data acquisition terminal; Photovoltaic Power Supply, MPPT, Conductor sag; Conductor tension

1 Introduction

The current ratings are based on the assumption that it is the worst combination of weather conditions which maintain the safe ground clearances of transmission line at all times. In fact the probability of co-incidence of the worst weather conditions is exceedingly small. In view of the risk of degradation of the material properties and of possible problems with grease leaking out of ACSR conductors and with sagging conductors [1], the margin conditions of conductor capacity including maximum permissible conductor temperature have been fixed for copper and for ACSR conductors in some countries (shown in table 1). The maximum permissible conductor temperature has been fixed at 90^0C for ACSR conductors in USA and Japan. It is fixed at 70^0C for ACSR conductors in China yet.

It is clear that the full utilization of the cooling of the ambient environment will allow higher circuit loading for short lines [2]. With the rapid economic growth, the electric power demand is urgent need, especially in China. Although the steps of power source construction speed up in recent years, the transmission capability of power grid is still prominently insufficient. Thermal capacity of transmission lines has been limited to a fixed (static) rate in case of the overheating problem when line load increases. But the operating experience shows that the limit value conservatively permits safe operation only under worst weather conditions (such as windless under high temperature). So it makes real time rating system possible using the real-time monitor of weather conditions and a complete series of line parameters.

Table 1 Margin conditions of conductor capacity in several countries

Boundary conditions	IEC	China	Japan	France	Indonesia	USA	UK		
							Winter	Ordinary day	Summer
Ambient temperature / ℃	35				35		5	20	35
Wind $(m \cdot s^{-1})$	1.0	0.5	0.5	1.0	0.5	0.61	0.45	0.45	0.22
Heat flux $(W \cdot m^{-2})$	900	1 000	1 000	900	1 250		850	850	1 050
Solar absorptivity	0.5	0.9	0.9	0.5		0.5	0.9	0.9	0.9
Emissity	0.6	0.9	0.9	0.6		0.5	0.9	0.9	0.9
Conductor temperature / ℃		70	90	85	75	90	15～100	30～120	50～120

The term dynamic rating refers to the utilization of real time information to develop accurate ratings of components. In the case of overhead transmission lines, the key elements in the development of a dynamic thermal rating are the conductor composition and construction, its temperature, the ambient temperature, the wind speed, and its direction. The dynamic thermal rating of an overhead conductor may be defined as the steady load that produces the maximum conductor operating temperature, computed on an instantaneous basis for actual loading and weather conditions [2].

Reference [3] indicates that the Short Term Emergency (STE) rating is a transient dynamic rating that considers the heat capacity of the conductor and the rise from the existing temperature to the limiting temperature. The maximum conductor temperatures for each rating are specified by the user. They are usually established by either the vertical ground clearance requirements (sag) or the annealing characteristic of the conductor. The Line's rating is taken as the lowest rating of all points considered.

The dynamic line rating (DLR) system designed in this paper can evaluate transmission capacity dynamically through measuring the real weather condition and monitoring the on-line parameters of over head lines. The technology using the existing transmission lines and relative devices increase line capacity without violating the legal ground clearance, and avoid unnecessary contingency accident. So taking the method at the lowest cost can delay to upgrade transmission line or to construct more lines, and save the limited soil resource.

2 Design of DLR system

2.1 Structure of the system

The DLR system is composed of data acquisition terminals installed on dead-end configuration of a line and one control instrument equipped in dispatch center. The data between the data acquisition terminals and the control instrument is transmitted through GPRS/GSM (Fig. 1).

Through Ethernet, the control instrument exchanges data with SCADA in order to integrate DLR and SCADA system. When the system operate normally, the control instrument receives real-time conductor tension, weather information and physics state of transmission lines from the data acquisition terminals, and obtains load current from SCADA system., then calculates conductor temperature and sags of line. Combining these data, the control instrument calculates line ratings, returns these results to the database of SCADA system, and displays the results on the operator screen.

Governing the line rating limits are the following three major limitations which insure the overhead transmission line operate safely:

1. Maintain adequate ground clearance. The system should provide operators advance warning of impending clearance violations, and insure the potentially minimum clearances to ground for safety reasons even under worst case conditions.

2. Limit the maximum allowable conductor temperature. The maximum allowable conductor temperature is normally selected so as to limit either conductor loss of strength due to the annealing of aluminum or to maintain adequate ground clearance.

3. Limit the allowable temperature of conductor junction. When lines are heavily loaded, the temperature of conductor junction is normally higher than that of conductor. In addition the matched hardware fittings should meet the request of safe operation under the heavily loaded conditions.

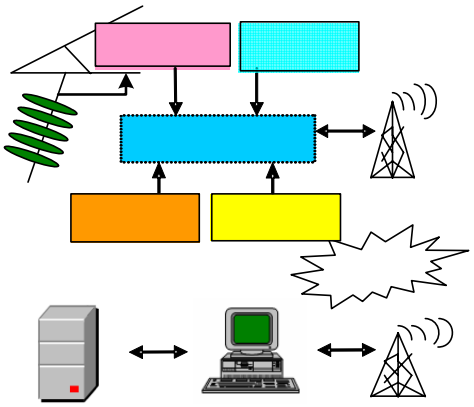

Fig.1 Structure of the system

2.2 Hardware and software design

The DLR system can achieve dynamical evaluation of the transmission capacity by measuring the actual weather condition related to line rating such as the wind speed, wind direction, ambient temperature and radiation temperature, and monitoring the real-time conductor tension, using this terminal based on MCU C8051F040.

The data acquisition terminal system based on MCU C8051F040 is designed to process the data by sampling, amplifying, filtering, processing, sending, and storing. The hardware diagram of data acquisition system is shown in Fig.2. Main function modules involve the microprocessor, the data acquisition, the data FLASH storage, the data wireless GPRS/GSM transmission, the real-time clock system and the communication with the power

management system module, and so on. Furthermore, the EMC (Electro Magnetic Compatibility) anti-interference of high voltage is solved by improving the software and hardware which are used in the system. The equipment has already past the related EMC tests. The power frequency magnetic field immunity test is shown in Fig. 3. The EMC test shows the good disturb resist ability of the DLR system. At present the DLR system has finished the test run phase, and has been put into operation in transmission lines in Guangzhou. The results of test run indicate that the performance of the system is in good condition, which meets the design requests.

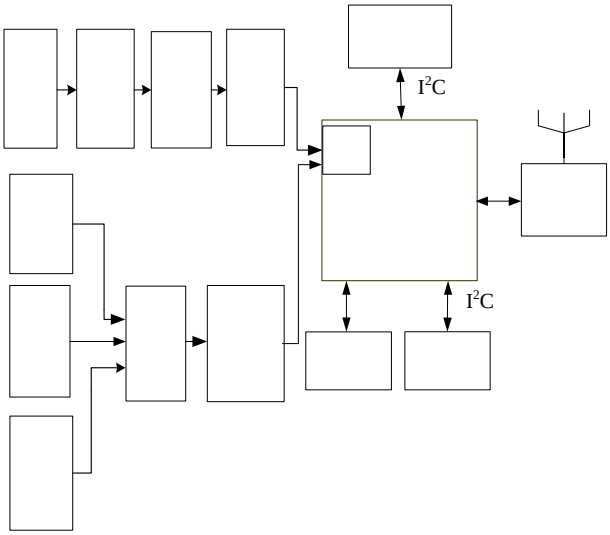

Fig.2 Hardware diagram of data acquisition system

Fig. 3 field test picture of power frequency magnetic field immunity test

Emphasis of Software part is to build the monitor management and data analysis system. In the building process, we first used user-case based techniques to analyze demands and capture concern, which is shown in Fig.4. Then add-in framework of SharpDevelop [4] is transplanted, based on which the module division is finally decided. Realizing of the modules while keeping them separate is difficult. We accomplished that via a newly developed .NET based aspect orient programming. Applying these techniques, the software is highly modulized and decouplized, which is very beneficial to redeveloping and transplantation.

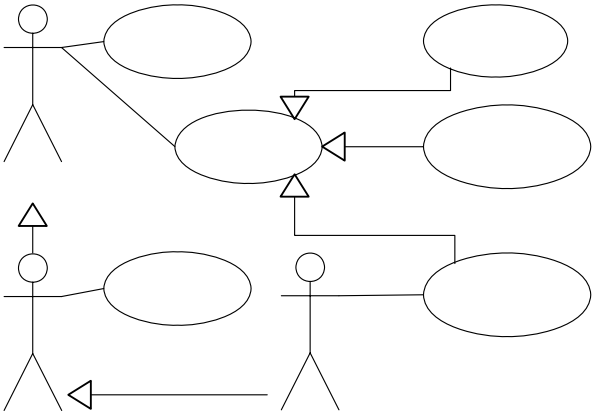

Fig.4 Application user-case diagram of DLR system

2.3 Design of Solar photovoltaic power supply system with multi-battery

2.3.1 PV model

Photovoltaic (PV) sources have the advantage of being maintenance and pollution-free. They are used today in many applications [5][6]. The conversion of solar energy into electric energy is performed by means of photovoltaic generators which supply electric current in the first quadrant of the current-voltage plane, particularly, in the voltage region located within the [0, V_{oc}] interval [7]. Fig.5 shows current-voltage and power-voltage characteristics of the photovoltaic array. PV array under uniform irradiance exhibits a current-voltage characteristic with a unique point P_m, called the maximum power point (MPP), where the array produces maximum output power [7]. The voltage power characteristic of photovoltaic array is not linear because of the variation which caused by a solar intensity and a temperature, and we cannot adopt the liner control theory easily to obtain the maximum power of the photovoltaic array [8].

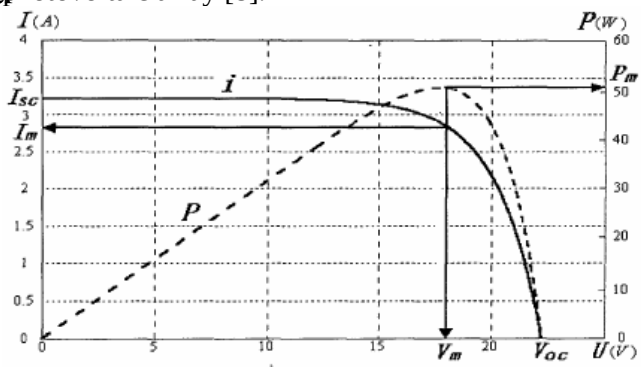

Fig.5 Current-voltage and power-voltage characteristics of the photovoltaic array

Maximum power point tracking (MPPT) techniques are used in PV systems to maximize the PV array output power by tracking continuously the maximum power point (MPP) which depends on panels' temperature and on irradiance conditions [9][10].

Among the various techniques proposed, the Perturb & Observe maximum power point tracking algorithm is the most commonly used method, due to its ease of implementation. It is based on the following criterion [11]: if the operating voltage of the PV array is perturbed in a given direction and if the power drawn from the PV array increases, this means that the operating point has moved toward the MPP and, therefore, the operating voltage must be further perturbed in the same direction. Otherwise, if the power drawn from the PV array decreases, the operating point has moved away from the MPP and, therefore, the direction of the operating voltage perturbation must be reversed.

We suppose that the system is working at steady-state [11], under constant and uniform irradiance level, and that the MPP has been reached. If the operating point of the PV array lies in a sufficiently narrow interval around the MPP, the power drawn by the PV array can be expressed as:

$$P(t) \cong \frac{v_{PV}^2(t)}{R_{MPP}} \quad (1)$$

Where $R_{MPP}=V_{MPP}/I_{MPP}$. V_{MPP} and I_{MPP} are the PV array MPP voltage and current, respectively.

The PV array power is the maximum when the adapted load resistance R equals the absolute value R_{MPP} of the differential resistance of the PV array at the MPP. In order to identify the minimum value to assign to T_a, the behavior of the system forced by a small duty-cycle step perturbation must be analyzed. In fact, in order to allow the MPPT algorithm to make a correct interpretation of the effect of a duty-cycle step perturbation on the corresponding steady-state variation of the array output power p, it is necessary that the time between two consecutive samplings is long enough to allow p to reach its steady state value.

The equivalent circuit of a PV array is shown in Fig.6. The relation between the array terminal current and voltage is the following:

$$I = I_L - I_o\left\{\exp\left[\frac{q(V+IR_S)}{AkT}\right]-1\right\}-\frac{V+IR_S}{R_{sh}} \quad (2)$$

Where

$$I_o = I_{or}[\frac{T}{T_r}]^3 \exp[\frac{qE_{GO}}{Bk}(\frac{1}{T_r}-\frac{1}{T})$$

$$I_{LG} = [I_{SCR} + K_I(T-25)]\lambda/100$$

Where q is electronic charge; k is Boltzmann's constant; λ is solar irradiation in W/m; I_{SCR} is short-circuit current at 25 and 1000 W/m^2; R_s is series resistance, which represents the resistance between the cells; R_{sh} is shunt resistances; I_L is the light induced current; A=B=1.92, is the diode ideality factor; I_o is the diode saturation current and V is the thermal voltage. The PV array current I is a nonlinear function of the PV array voltage V, of the irradiance level S and of the temperature T [11].

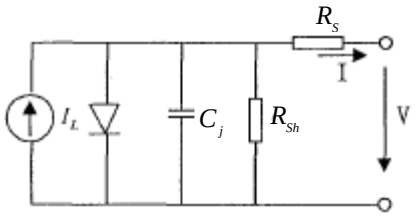

Fig.6 Equivalent circuit of photovoltaic array

The temperature changes affect mainly the PV output voltage, while the irradiation changes affect mainly the PV output current. The intersection of the load-line with the PV module I-V characteristic, for a given temperature and irradiation, determines the operating point. The maximum power production is based on the load-line adjustment under varying atmospheric conditions [12].

2.3.2 Solar photovoltaic power supply system

The battery management system (shown in Fig.7) is a solar photovoltaic power supply system for DLR on-line monitoring system. It includes the capacity selection for PV array, rechargeable battery pack, maximum power point tracking for PV array, charge and discharge method for battery pack. Under different temperature and light intensity, MPPT strategy can always obtain the highest possible power from PV array, which ensures the charge efficiency of battery pack. The charge and discharge method effectively extend the life of battery pack. Designed and realized the I^2C line agreement which was used to communicate between the CPU of the power supply system and the CPU of the data acquisition system. The capacity of PV array and battery was selected according to the need of the power consumption of devices and the weather condition.

In this DLR power supply system, choose parameters as follows: short circuit current Isc=0.92A, open-circuit voltage Voc=22V, the current at MPP I_m=0.83A, the voltage at MPP V_m=18V, the MPP P_m=15W.

Fig.8 shows the experimental result of the output voltage of PV power supply system under the condition that the solar cell array is in the sun. Operational results show that the PV power supply

system has the characteristic of high stability and high efficiency.

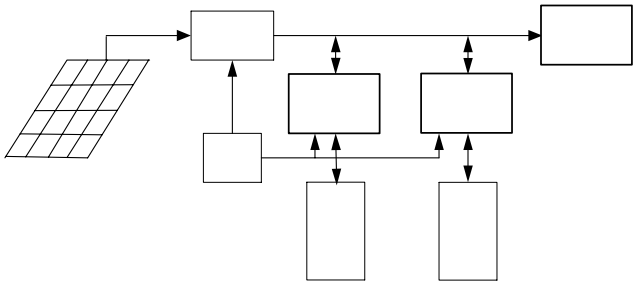

Fig.7 Diagram of battery with grouping management

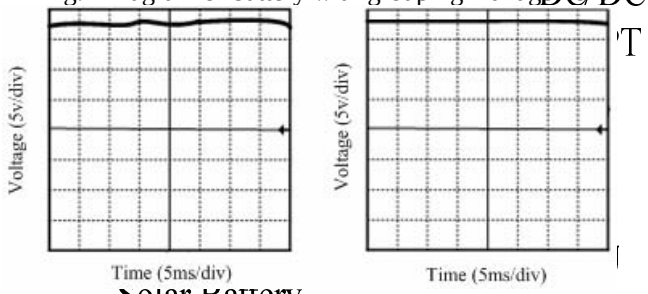

Fig.8 Experimental result of PV power supply system. (a) Output voltage without MPPT; (b) Output voltage with the proposed MPPT method.

3 Principles of DLR system Conclusion

3.1 Rating calculation

The dynamic thermal rating of an overhead line conductor is described by heat balance equation [13]-[16]. The relation is shown below in equation (3).

$$I^2*R(Tc)+Q_s=M\cdot Cp\cdot dTc/dt+Q_c+Q_r \quad (3)$$

During steady-state conditions, the equation is:

$$I^2*R(Tc)+Q_s=Q_c+Q_r \quad (4)$$

Where Q_c is the convective loss,(W/m^2); Q_r is the radiated heat loss, (W/m^2); Q_s is the solar heat , (W/ m^2);M is the mass of the conductor ,(kg/m); *Cp* is the specific heat of conductor, (J/(kg℃)); T_c is conductor temperature,(℃); *R(Tc)* is the ac resistance of conductor,(ohm/m).

The electrical resistance of bare stranded conductor varies with frequency, average current density, and temperature. A simple method to calculate resistance at *Tc* is as shown in Equation (5).

$$R(T_c)=(1+k)R_d \quad (5)$$

Where R_d is AC resistance at *Tc*; R_{20} is AC resistance at 20℃; α_{20} is temperature coefficient of resistance; k is coefficient of skin effect.

$$R_d = R_{20}[1+\alpha_{20}(T_c-20)]$$

The steady-state thermal line rating equation of the conductor is shown:

$$I=[\frac{Q_c+Q_r-Q_S}{R(T_C)}]^{\frac{1}{2}} \quad (6)$$

3.1.1 Convection heat loss

Line capacity is most affected by the wind (cooling effects) and load (heating effects) on the line. The convective heat loss, Q_c, is a function of wind speed, direction and conductor temperature rise above air temperature.

Wind is more important than all the other factors which affect conductor capacity [15]. Wind speed increases, which will enhance the convective heat loss, and increase the line capacity finally.

With zero wind speed, natural convection occurs, where the rate of heat loss is as shown in Equation (7).

$$Q_{c0}=0.0205\rho_f^{0.5}D^{0.75}(T_c-T_a)^{1.25} \quad (7)$$

It has been argued that at low wind speeds, the convection cooling rate should be calculated by using a vector sum of the wind speed and a "natural" wind speed, see Morgan equation. However, it is recommended that only the larger of the forced and natural convection heat loss rates be used at low wind speeds instead of their vector sum as this is conservative.

When it is at low winds and at high winds, Forced convection heat loss rate is shown as follows:

$$Q_{c1}=\left[1.01+0.0372\left(\frac{D\rho_f V_w}{\mu_f}\right)^{0.52}\right]k_f\times (T_c-T_a)k_{angle} \quad (8)$$

$$Q_{c2}=0.0119\left(\frac{D\rho_f V_w}{\mu_f}\right)^{0.6}K_f(T_c-T_a)k_{angle} \quad (9)$$

Where ρ_f is air density, (kg/m^3), μ_f is air viscosity, (kg/m•s); k_f is coefficient of thermal conductivity of air, (*w/m*℃); D is conductor diameter.

$$\mu_f=\frac{1.458\times10^{-6}(T_{film}+273)^{1.5}}{T_{film}+383.4}$$

$$K_f=0.02424+7.4767\times10^{-5}T_{film}-4.4071\times10^{-9}T^2_{film}$$

$$\rho_f=\frac{1.293-1.525\times10^{-4}H_e+6.397\times10^{-9}H_e^2}{1+0.00367\times T_{film}}$$

$$T_{film}=(T_c+T_a)/2$$

Equation (8) applies at low winds but is too low at high speeds. Equation (9) applies at high wind speeds, being too low at low wind speeds. At any wind speed, the larger of the two calculated convection heat losses is used. The convective cooling term is multiplied by the wind direction factor, K_{angle}, where ϕ is the angle between the wind direction and the conductor axis:

$$K_{angle} = 1.194 - \cos(\phi) + 0.194\cos(2\phi) + 0.368\sin(2\phi) \quad (10)$$

$$Q_c = Maximum(Q_{c0}, Q_{c1}, Q_{c2}) \quad (11)$$

For a given wind speed, winds blowing parallel result in a 60% lower convective heat loss than winds blowing perpendicular to the conductor.

Effects of wind turbulence and conductor stranding appear to be of minor importance in thermal rating or conductor temperature calculations. Evaporative cooling is a major factor, but it occurs sporadically along transmission lines. Both are neglected in this standard.

Reference [16] indicates proposed that a primary concern or caution must involve the choice of wind speed and direction, because the wind is normally assumed to be perpendicular to the conductor axis for rating calculations. Several cautions are included with regard to the proper choice of weather conditions for thermal line rating calculations with bare overhead conductors.

(1) There is considerable evidence from field measurement that still air conditions can exist over limited lengths of line for periods of up to several hours particularly near sunset and sunrise. During periods of still air, convective cooling of the conductor is limited to natural convection, which is equivalent to forced convection at a wind speed of 0.2 m/s.

(2) Measurements of wind speeds at a single location will always indicate higher average and minimum wind speeds than simultaneous measurements of wind speed at multiple locations along a transmission line. Thus indications of wind speed from measurements at a single location are usually a poor basis for line ratings since it is likely that wind conditions are less favorable at another location along the line.

(3) Convective cooling of a bare overhead conductor is dependent on both the wind speed and wind direction. A perpendicular wind speed of 0.6 m/s even could yield the same convective cooling as a wind of 1.3 m/s at an angle of 22.5°. Thus, when choosing an appropriately conservative wind speed for thermal rating calculations, both the angle and the wind speed should be considered. The conventional assumption of perpendicular wind flow is not conservative.

3.1.2 Radiated heat loss

The radiated heat loss, Q_r, is a function of conductor temperature rise above air temperature, and conductor characteristic, such as emissivity, inner structure and diameter, etc. It is calculated by Equation (10).

$$Q_r = \pi D\varepsilon\sigma[(\frac{T_c + 273}{100})^4 - (\frac{T_c + 273}{100})^4] \quad (12)$$

Emissivity ε and absorptivity α increase from about 0.2 to about 0.9 with age. The exact rate of increase depends on the level of atmospheric pollution and the line's operating voltage. α is generally higher than ε over the life of the conductor. Both values increase with age and atmospheric pollution. Values of 0.5 for both absorptivity and emissivity, or 0.9 for absorptivity and 0.7 for emissivity, have been used when the actual conductor surface condition is unknown [16].

3.1.3 Solar heat gain

The solar heat, Q_s, being absorbed by the conductor is a function of the conductor absorptivity, line latitude and evaluation above sea level, and the relative solar angles of the conductor. A simple method for the calculation of solar heat gain is provided by Equation (10) and (11).

$$Q_S = \alpha q_S \sin(\theta) A' \quad (13)$$

Where θ is effective angle of incidence of the sun's rays; Hc is altitude of sun; Zc is azimuth of sun; Z_l is azimuth of line.

$$\theta = \cos^{-1}[\cos(H_C)\cos(Z_C - Z_l)]$$

The most conservative results are obtained by assuming an angle of incidence of 90°, which will give the lowest value of ampacity and will be appropriate for many purposes.

Solar heat input to a bare overhead conductor can cause a conductor temperature rise above air temperature of up to 15 °C in still air. However, more typically, periods of maximum solar heat input are associated with significant wind activity and the actual temperature rise measured for bare conductors in overhead transmission lines seldom exceeds 5 °C to 10 °C [15].

3.2 Mechanical analysis of transmission lines and sag calculation

Overhead transmission lines operate at high voltages, so they must meet certain legal ground clearances at all times to insure safe operation. Sag

is an important design and operation parameter of a transmission line. The tension of line determines the sag at all times. The tension monitors were installed between dead-end insulators and the dead-end structure. Transmission line spans are catenary curves. Given the tension, the sag in a dead-end span may be calculated using a conventional catenary equation with little error.

The ruling span and the ruling difference angel are used in the convective spans. The ruling span formula is based on the fundamental assumption that the attachments of the conductor to suspension structures between dead-end structures are flexible enough to allow for longitudinal movement to equalize the tensions in adjacent spans to the ruling span tension [17][18]. The ruling span length RS is:

$$RS = \sqrt{(\sum_{1}^{n} l_i^{3} \cos\beta_i)/(\sum_{1}^{n} l_i / \cos\beta_i)} \qquad (14)$$

Where i is the number of spans; l_i is Span length; β_i is the angle of inclination, $\beta_i = tg^{-1}(h_i/l_i)$; h_i is the difference in height between two terminal point of one span.

The ruling difference angel of the convective spans is:

$$\cos\beta = (\sum l_i / \cos\beta_i)/(\sum l_i / \cos^2\beta_i) \qquad (15)$$

The wind varies with space and with time, and is not unpredictable. Even though wind blew perpendicular to the conductor, the conductor would deflect the initial position, which came into being an angle between the wind direction and the conductor axis (Fig.9). Because of the sags, the angles are different along the line, and the wind pressures perpendicular to the conductor are also different, which complicate the calculation.

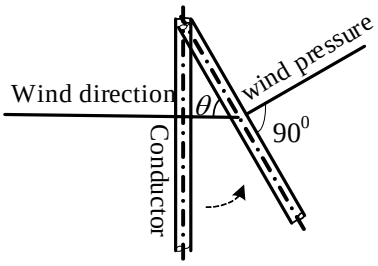

Fig.9 Deflection of conductor blowing by wind

The ratios of sag to span length and line length to inclined span length l_{AB} (Fig.10) which is the distance between two adjacent points of conductor are very small for overhead transmission line [17]. It is on the assumption that the angle θ between wind direction and the conductor axis is constant in the same span. The value of θ is equal to that of the angle between wind direction and the inclined span l_{AB}, i.e. neglect the action what sags and line deflection influence θ and pressure perpendicular to the conductor. So it is approximately considered that the pressure perpendicular to the conductor is well-distributed along the inclined span, and defined as γ_h. And the composition of force $\gamma' = \sqrt{\gamma_v^2 + \gamma_h^2}$, where γ_v is the weight of conductor.

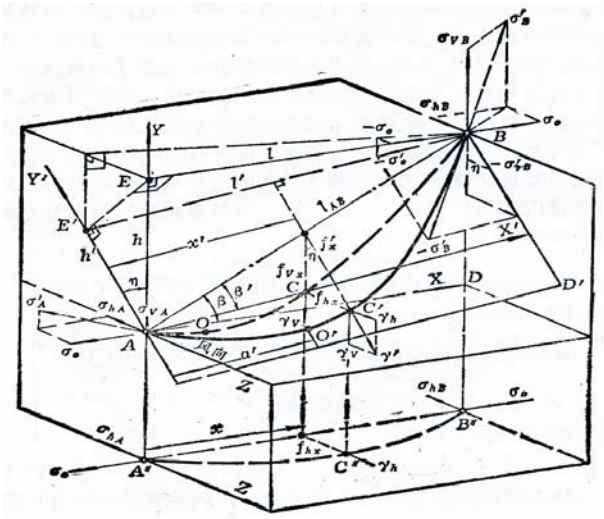

Fig.10 Force balance for overhead line in wind

When line deflects initial position because of the action of wind, it must be situated in the inclined plane ABC'D'E' which composition of forces is in. The line located in vertical plane ABCDE without wind. When line is blown by wind, one point of line C located in vertical plane act along with wind and move to C', until the torque relative to the axis AB lessen to zero. So the angle of line deflection η is defined as the angle between the composition of forces and the vertical line, which is calculate using the following equation.

$$\sin\eta = \frac{\gamma_h}{\gamma'}, \cos\eta = \frac{\gamma_v}{\gamma'}, \tan\eta = \frac{\gamma_h}{\gamma_v} \qquad (16)$$

According to the geometrical Fig.3, the relationship of the parameters in line deflection plane to the parameters in vertical plane can be calculated.

$$l' = l\sqrt{1+(\tan\beta\sin\eta)^2}$$

$$\sigma_0' = \sigma_0\sqrt{1+(\tan\beta\sin\eta)^2}$$

$$\cos\beta' = \cos\beta\sqrt{1+(\tan\beta\sin\eta)^2}$$

$$h' = h\cos\eta$$

The forces of suspension A and suspension B in deflection plane is calculate using the following equation.

$$\sigma_{\gamma A}' = \frac{\gamma'}{\cos\beta'}\left(\frac{l'}{2} - \frac{\sigma_0' h' \cos\beta'}{\gamma' l'}\right) \qquad (17)$$

$$\sigma_{\gamma B}^{'}=\frac{\gamma^{'}}{\cos\beta^{'}}\left(\frac{l^{'}}{2}+\frac{\sigma_0^{'}h^{'}\cos\beta^{'}}{\gamma^{'}l^{'}}\right) \quad (18)$$

$$\sigma_{\gamma A}^{'\,2}+\sigma_0^{'\,2}=\sigma_A^{'\,2} \quad (19)$$

The measured tension $T_A=\sigma_A^{'}*S$

Where S is cross sectional area (m^2) of conductor. So the horizontal force in the deflection plane is:

$$\sigma'_0=\sqrt{(\frac{T_A}{S})^2-\sigma'^2_{\gamma A}} \quad (20)$$

The sag of any point C' can be monitored:

$$f_x'=\frac{\gamma' x(l-x)}{2\sigma_0\cos\beta_i} \quad (21)$$

When the suspension point in height is equal, i.e. the angle of inclination β is zero, the horizontal forces in deflection plane is equal to that in vertical plane. In this occasion the calculation would be simplified greatly. Maximum sag in the midpoint of the span is:

$$f_M^{'}=\frac{\gamma^{'}l'^2}{8\sigma_0^{'}\cos\beta^{'}} \quad (22)$$

The sags of the spans can be calculated:

$$Di=(\frac{li}{RS})^2\times\frac{\cos\beta}{\cos\beta_i}\times D \quad (23)$$

3.3 Conductor temperature calculation

Conductor temperature can be calculated using by state equation of overhead transmission line. The horizontal forces could be calculated from tensions value under certain conditions.

$$\sigma_n-\frac{l'^2g_n'^2E}{24\sigma_n^{\,2}}\cos^3\varphi=\sigma_m-\frac{l^2g_m^{\,2}E}{24\sigma_m^{\,2}}\cos^3\varphi- \quad (24)$$

$$\alpha E(t_n-t_m)\cos\varphi$$

Where t_n and $t_m$are temperatures of conditions n and m respectively; $\sigma_n$and σ_m are horizontal forces of the conductor under conditions n and m; E is elastic coefficient of the conductor, (N/mm^2); α is temperature coefficient of the conductor, ($℃^{-1}$).

The ruling span l' of consecutive spans in wind conditions is calculated using equation (12).

Some of experience verified the relationship of the sag to the temperature of a homogenous conductor is almost linear [19]. It can correct the values which equation calculated.

$$l'=\frac{\sum_1^n l_i/\cos^2\varphi_i}{\sum l_i/\cos\varphi_i}\sqrt{\frac{\sum l_i^{\,3}\cos\varphi_i(1+tg^2\varphi_i\sin^2\eta)}{\sum l_i/\cos\varphi_i}}$$
$$=\frac{1}{\cos\varphi}\sqrt{\frac{\sum l_i^{\,3}\cos\varphi_i(1+tg^2\varphi_i\sin^2\eta)}{\sum l_i/\cos\varphi_i}} \quad (25)$$

3.4 Thermal model for rating calculation

Three models to dynamic rating have been proposed in recent years: WM (weather-base model), CTM(conductor temperature model), and TS(tension-sag model). WM and CTM are traditional models to rate capacity of conductor, as per [3][20].

(1)WM(weather-based model)

The weather-based method calculate the capacity of conductor from conductor current and weather parameters based on IEEE 738-93 standard. These weather parameters data may be obtained from local weather station at relatively low cost. Besides, the data for the latitude and elevation of conductor above sea level, and atmosphere index is necessary.

The system depends on software mainly and does not require installing additional transmission line hardware and conductor temperature sensors. The disadvantage of it is susceptible to error resulting from variation of the terrain and forecasting of weather patterns.

(2)CTM(conductor temperature model)

This method based direct temperature measurement measures the surface temperature of conductor on different spans [3], which is described in equation (13). The condition is limited at low wind speeds, and the load current is high enough to measure the temperature accurately.

$$M\,C_p\,dT_c/dt+Dh(Tc-Ta)+Q_r=I^2\times R(Tc)+Q_s \quad (13)$$

Where *h(t)* is connective heat transfer coefficient.

The primary drawback of the CTM approach is that under low current load conditions the conductor temperature error becomes increasingly significant.

(3) TS(tension-sag model)

When conductor temperature, load, weather, heat dissipation and aging varied, the sags of transmission line would correspond to vary, which result variation of conductor tension. The method based tension monitors rates the conductors using above relationship.

The relationship between conductor temperature and sag in a dead-end section could be established when the locations and characteristic of conductor were known. The tension based method installs tension monitors between the dead-end insulators, calculate the average temperature of sections, and rate the conductors.

TS model is a relatively new model to calculate line capacity. In order to make sure the model to function accurately, the load must produce 5 degrees temperature rise. The accuracy increases when the conductor temperature rises [21].

WM and CTM are traditional models to rate capacity of conductor. The major difference between them is the calculation of heat transfer coefficient *h(t)*. WM calculate the coefficient from air temperature, wind speed and direction. So it is more accurate when wind speeds are high.

In the case of CTM, the heat transfer coefficient is obtained directly from the measured temperature and conductor current. The CTM method lacks accuracy when the conductor is not heavily loaded or the conductor temperature rise over ambient is small under the high cooling conditions. A conclusion derived from reference [19] stated when the conductor temperature rises over ambient is less than 10 degrees, the WM ratings are consistently more accurate than the CTM ratings.

Combined above statement, the system select TS model when the line is sufficiently loaded to rate the conductors, otherwise the WM model is selected.

4 Test and analysis

Fig.11 shows the calculated rating of a line in typical 24 hour. The curve 1 is a daily load curve. The straight line is calculated static rating. From Fig.6, the TS based rating is even below the static rating and cannot function when the line load is so low at night. WM is more accurate and applied to rate the capacity of the line when conductor temperature rise over ambient is small. The system select TS based rating when the line is sufficiently loaded to rate transmission line, otherwise the WM based model is selected. The result demonstrates that the real-time rating is relative stable, and it could be as much as 150 percent more than the normal rating.

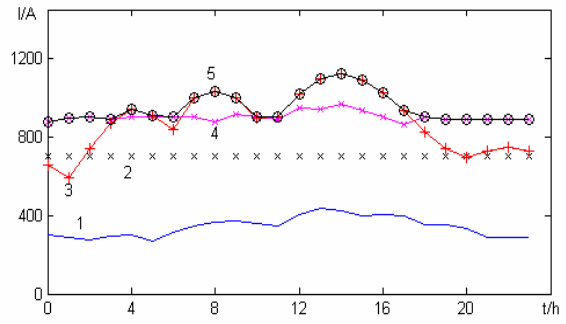

Fig.11 Curve of real-time rating.

1.Load of a transmission line;2. Static rating; 3. Rating calculated by TS model; 4. Rating calculated by TS model; 5. Real time rating.

5 Conclusion

The DLR system that can evaluate transmission capacity dynamically through measuring the real-time conductor tension and weather information is designed in the paper. DLR technology increase line capacity dynamically without violating the legal ground clearance, and monitor the on-line parameters of transmission lines, which avoid unnecessary contingency accident and insure safe operation.

Perturb & Observe MPPT techniques are used in photovoltaic systems to maximize the PV array output power by tracking continuously the MPP. Battery grouping and the charge and discharge strategy, as an innovation in the design of the power supply system, were proposed and realized. The operation results show that perturb & observe methods excellently realize the MPPT, improve the charging efficiency of the PV array, battery grouping and the charge and discharge management extend the life of battery pack.

The force balance for overhead line in wind was analyzed in detail, which deduces the mechanical model to calculate sags from the measured tension. The system can monitor the sags of each spans and the average temperature of conductor, which insure the safe ground clearances at all times.

This paper compared the advantages and drawbacks of the mathematic models used to calculate transmission capacity, and combined the WM and TS model in the paper. The force balance for overhead line in wind was analyzed in detail, which deduces the mechanical model to calculate sags from the measured tension. The system can monitor the sags of each spans and the average temperature of conductor, which insure the safe ground clearances at all times. The result shows that the DLR system is effective in increasing line capacity to 50 percent over the normal rating. The advantage of the system is low cost with high accuracy.

The function of the system was realized though the cooperation of the companions in the laboratory and the equipment had run in some transmission line in the southern power grid company. The results show that the equipments function very well and totally met the application need.

The anti-interference of high voltage is solved by improving the software and hardware which are used in the system. The suggestion, that measuring and reliable control technology used in power system should be applied to improve the transmission capacity of the lines for the system security, is proposed.

References:

[1] G.M.L.M. van de Wiel, A new probabilistic approach to thermal rating overhead-line conductors evaluation in the Netherlands, International Conference on Overhead Line Design and Construction, London, 1988, pp. 17-21.

[2] Holbert, K. E., Heydt, G. T, Prospects for dynamic transmission circuit ratings, The 2001 IEEE International Symposium on Circuits and Systems, Vol 3, 2001, pp. 205-208.

[3] Engelhardt, J.S., Basu, S.P., Design, installation, and field experience with an overhead transmission dynamic line rating system, Proceedings of the IEEE Power Engineering Society Transmission and Distribution Conference, Los Angeles, 1996, pp. 366-370.

[4] C. Holm, M.K., B. Spuida, *Dissecting a C# Application Inside SharpDevelop*, Wrox, 2003.

[5] Benmohamed, Zohra, Remram, Mohamed, Effect of growth process on polycrystalline silicon solar cells efficiency, WSEAS Transactions on Electronics, Vol.3, No.4, 2006, pp. 253-257.

[6] Theodoridis, Michael P., Axaopoulos, Petros, Architecture and performance of a power management system for multiple compressor solar ice-makers, WSEAS Transactions on Systems, Vol.6, No.4, 2007, pp. 823-830.

[7] Leyva, R., Alonso, C., Queinnec, I., et al, MPPT of photovoltaic systems using Extremum–Seeking Control, IEEE Transactions on Aerospace and Electronic Systems, Vol.42, No.1 2006, pp.249 – 258.

[8] Kasa N., T. Iida, G. Majumdar, Robust control for maximum power point tracking in photovoltaic power system, Proceedings of the PCC, Osaka, 2002, pp.827-832.

[9] Femia , N. Optimizing Duty-cycle Perturbation of P&O MPPT Technique, Annual IEEE Power Electronics Specialists Conference, 35th, 2004, pp. 1939-1944.

[10] Majin, Reza Ahmadian,Gharaveisi, A.A., et al, Speed improvement of MPPT in photovoltaic systems by fuzzy controller and ANFIS reference model, WSEAS Transactions on Circuits and Systems, Vol.5, No.8, 2006, pp. 1238-1243.

[11] Femia N., Optimization of perturb and observe maximum power point tracking method, IEEE Transaction on Power Electronics, 2005, Vol.20, No.4, pp. 963-973.

[12] Eftichios Koutroulis, Kostas Kalaitzakis, Nicholas C. Voulgaris, Development of a Microcontroller-Based, Photovoltaic Maximum Power Point Tracking Control System, IEEE Transaction on Power Electronics, 2001, Vol.16, No.1, pp. 46-54.

[13] Liu Sheng, Foundation of Electric Engineering, Beijing Science Press, 2002.

[14] IEEE Standard 738-1993, IEEE standard for calculating the current-temperature relationship of bare overhead conductors, USA: The Institute of Electrical and Electronics Engineers, Inc., 1993.

[15] Tapani O.Seppa, A practical approach for increasing the thermal capabilities of transmission lines, IEEE Transactions on Power Delivery, Vol.8, No.3, 1993, pp.1536-1542.

[16] IEEE Standard 738-2006, IEEE standard for calculating the current-temperature of bare overhead conductors, USA: The Institute of Electrical and Electronics Engineers, Inc., 2007.

[17] Shao Tian-xiao, Design of over-head transmission lines, Beijing: China Electric Power Press, 1987.

[18] Y. Motlis et al., Limitations of the ruling span method for overhead line conductors at high operating temperatures, In Report of the IEEE Task Force “Bare conductor sag high temperature”, IEEE/PES Winter Meeting, 1998.

[19] Raniga, J.K., Rayudu, R.K., Dynamic rating of transmission lines-a New Zealand experience, Power Engineering Society Winter Meeting, 2000, pp. 2403-2409.

[20] Stephen D. Foss, Robert A. Maraio, Dynamic line rating in the operating environment, IEEE Transactions on power Delivery, Vol.5, No.2, 1990, pp. 1095-1105.

[21] Seppa, Tapani O., Accurate ampacity determination: Temperature-sag model for operational real time ratings, IEEE Transactions on Power Delivery, Vol.10, No.3, 1995, pp. 1460-1470.